A STUDY ON THE EFFECT OF NANO-PRECIPITATES ON FRACTURE BEHAVIOR OF NANO-STRUCTURED Al-2wt%Cu ALLOY FABRICATED BY ACCUMULATIVE ROLL BONDING (ARB) PROCESS

B. Azad[a,*], E. Borhani[b]

[a] Faculty of Metallurgical and Materials Engineering, Semnan University, Semnan, Iran
[b] Nano-materials Group, Department of Nanotechnology, Semnan University, Semnan, Iran

Abstract

An Al-2wt%Cu alloy was subjected to accumulative roll bonding (ARB) process up to a strain of 4.8. The two kinds of different microstructures, i.e, solution treated (ST) one and 190°C pre-aged for 30 min (Aged), were prepared as the starting structures for the ARB process. The microstructures were studied by transmission electron microscope (TEM) and electron backscattering diffraction (EBSD). The results showed that the fine precipitates having the average particle size of 16 nm were formed after aging process. On the other hand, the mean grain size of the ST-ARB and the Aged-ARB specimens reached to 650 nm and 420 nm, respectively. Study of the fracture surfaces were carried out by scanning electron microscope (SEM). The results indicated that at 0-cycle ARB, the specimens show dimples indicating the micro-void coalescence (MVC) mechanism of ductile fracture. The average size of dimples was larger in the ST-ARB specimen compared to the Aged-ARB specimen. The fracture mode was transgranular cleavage fracture in the Aged-specimen. At 3-cycle and 6-cycle ARB, also the specimens showed cleavage facets and river lines, that the river lines or the stress lines are steps between cleavage or parallel planes, which are always converged in the direction of local crack propagation.

Keywords: Al-2wt%Cu alloy; accumulative roll bonding (ARB) process; Fracture behavior; nano-precipitates.

1. Introduction

Interest in the processing of bulk ultrafine grained (UFG) materials through the application of severe plastic deformation (SPD) has significantly grown [1-5]. Several SPD techniques have been designed for achieving to high strength metals with minimal changes in the initial sample dimensions. Some SPD techniques, such as equal channel angular pressing (ECAP) [2], high pressure torsion (HPT) [3], cyclic extrusion compression (CEC) [4] and accumulative roll bonding (ARB) [5] have been developed. Among these SPD techniques, the ARB process allows to accumulate very large plastic strains into materials without changing the dimensions of the materials by repeating the process of cutting the rolled sheet, stacking them to be the initial thickness and roll-bonding the stacked sheets again [5].

The microstructure evolution, mechanical properties and texture evolution of ARB-processed alloys have been studied by many researchers [6-10], however, some characteristics of ARB-processed alloys such as fracture surfaces study still need an in-depth research. The fracture study is important to clarify the rupture mechanisms in the ARB processed specimens. Types of fracture can be described by transgranular fracture and intergranular fracture [11]. Transgranular fracture can be classified into brittle cleavage fracture, ductile fracture and fatigue fracture. Also, intergranular fracture can be classified into intergranular fracture without micro-void and intergranular fracture with micro-void. Brittle fracture occurs by either transgranular or intergranular cracking [11].

The binary Al–Cu system is a well-studied precipitation strengthening system because it forms the basis for a wide range of age-hardening alloys that are technologically important [12]. In the present study, the ARB process was carried out on Al-2wt%Cu alloy having different starting microstructures in order to research on the fracture behavior of the alloy during the ARB process. The aim of this study is to investigate of fracture behavior of solution treated (ST) and pre-aged specimens during the ARB process.

2. Experimental Procedure

An Al-2wt%Cu alloy was prepared as sheets with thickness of 2 mm, width of 60 mm and length of 200

* Corresponding author: Bahramazad1987@gmail.com

mm. Chemical composition of the material used in the present study is presented in Table 1.

Table1. *Chemical composition of Al-2wt%Cu alloy*

Alloying elements	Cu	Mg	Fe	Si	Mn	Cr	Ti	Al
Wt. %	1.96	0.001	0.022	0.004	0.001	0.006	0.0001	base

The sheets were solution-treated at 550°C/6hr and immediately quenched in the water. Some of the ST sheets were aged at 190 °C for 30 min, to have very fine Al_2Cu precipitates. These two types of sheets were used as the starting materials for the ARB process. The starting sheets with thickness of 2 mm were firstly cold-rolled by 50% reduction in thickness that named as the first ARB cycle. The 50% rolled sheets 1 mm thick were cut into two pieces. To prepare of sheets and create a satisfactory bond in the ARB process, the surfaces of the sheets were cleaned by acetone and were roughened by a wire brush and then roll-bonded by 50% reduction in one pass at room temperature as shown in Fig. 1. The same procedures were repeated up to 6 cycles including the first cold-rolling, which corresponded total equivalent strain of 4.8. The ARB process was carried out immediately to avoid for any oxide formation. The ARB process was carried out by two mills with 110 mm diameter rolls having rolling speed of 29 rpm. Thermal and mechanical procedures used in this study are schematically shown in Fig. 2. The solution treated specimen and the aged specimen after ARB process are denoted as ST-ARB and Aged-ARB specimens, respectively.

Sections normal to the transverse direction (TD) of the sheets were used for the microstructural observations. Electron backscattering diffraction (EBSD) analysis was carried out in a scanning electron microscope (SEM) with a field emission type gun (FE-SEM; Philips XL30) operated at 15 kV. The specimens were mechanically polished and then electro-polished in a solution of 30% HNO_3 and 70% CH_3OH before the measurements. The transmission electron microscope (TEM) observations were carried out using Hitachi H-800 operated at 200 kV. Thin foil specimens normal to TD were prepared through mechanical polishing firstly down to approximately 70 μm in the thickness, and then electro-polishing in the same solution as that for the EBSD specimens. The tensile test was carried out by strain rate approximately $10E-4S^{-1}$. On the other hand, fracture surfaces of the specimens after tensile test were investigated by SEM during the ARB process.
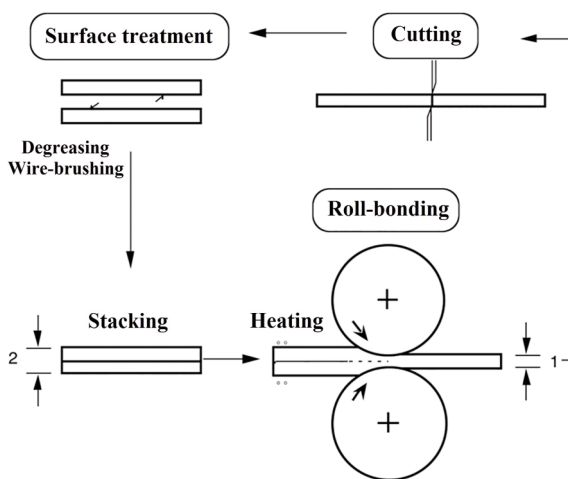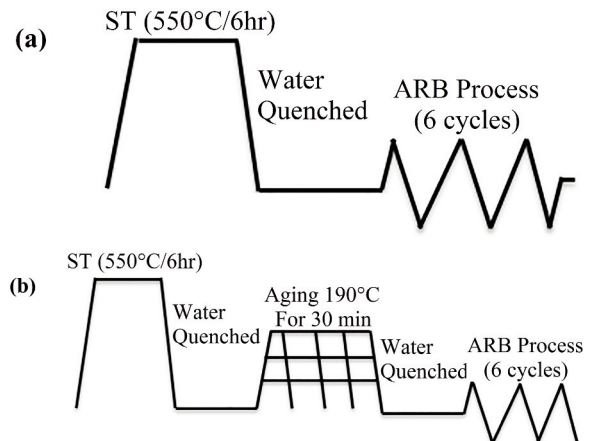
Figure 2. *Schematic illustration of a) ST-ARB and b) Aged-ARB processes*

3. Results and Discussion
3.1. Microstructure evolution

TEM micrograph of the Aged-specimen before the ARB process is shown in Fig. 3. Because the diffraction spots of Al_2Cu precipitates is very weak, it is difficult to know the orientation of these Al_2Cu precipitates. Therefore, Ashby-Brown contrasts [13,14] are used to understand the degree of coherency between a particle and the matrix. The Ashby and Brown contrast consists of spherical strain lines and irregular strain lines. The Ashby and Brown contrast appears around a spherical coherent precipitate in bright-field images. Loss of spherical strain caused by the introduction of interfacial dislocations is detected by the irregularity of the strain lines in the Ashby-Brown contrast. It is well known that the spherical strain lines appear around

Figure 1. *Schematic illustration of ARB process [5]*

a spherical coherent particle, whereas irregular strain lines appear inside a semi-coherent. As shown in Fig. 3, there are fine Al_2Cu precipitates indicated by arrows, having the average particle size of 16 nm, after aging process. Grain boundary maps obtained from EBSD analysis of the ST-ARB and the Aged-ARB specimens are shown in Fig. 4. The mean grain size is evaluated as the mean spacing of high angle grain boundaries (HAGBs) along normal direction (ND) by linear intercept method in the EBSD boundary maps. From the figure, the mean grain size of the samples reaches to 650 nm and 420 nm for the ST-ARB and the Aged-ARB specimens after 6-cycle ARB, respectively.
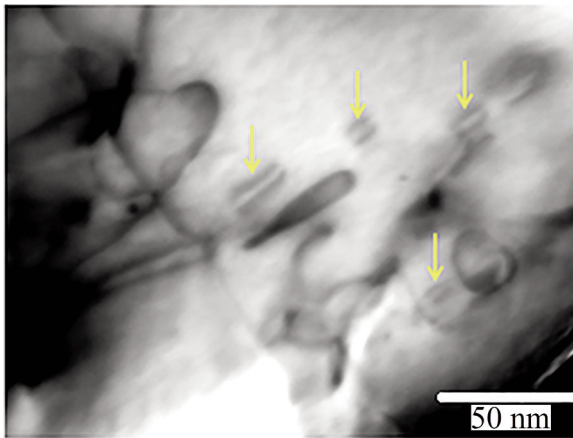
Figure 3. *TEM micrograph of the Aged-specimen before the ARB process showing the fine precipitates.*
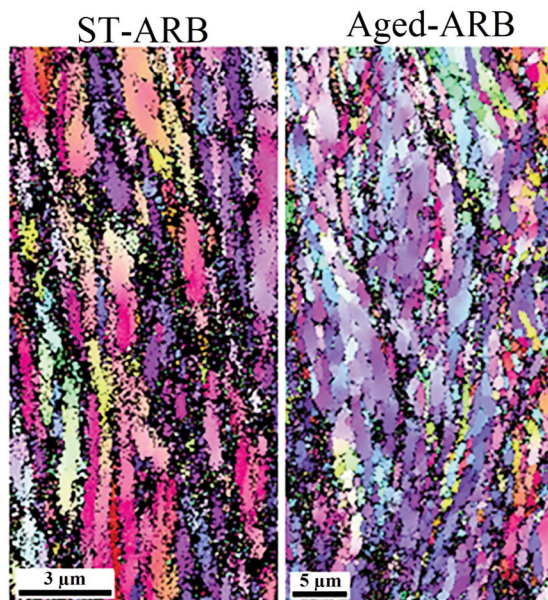
Figure 4. *Grain boundary maps obtained from EBSD measurements for the ST-ARB and Aged-ARB specimens after 6-cycle ARB*

3.2. Fracture behavior

Types of fracture can be roughly divided into two categories, which are brittle and ductile fractures [11]. Ductile and brittle describes the amount of macroscopic plastic deformation that precedes fracture [15]. Ductile fracture occurs by micro-void formation and coalescence. The former has however gained a lot of interests due to its catastrophic results whenever happens. In this case, some brittle fracture by crack propagation around its girth has been reported [16]. Limited amount of plastic deformation occurring during brittle fracture, promotes a sudden failure without warning. Ductile fracture on the contrary exhibits rough and dull fracture surfaces with gross plastic deformation, therefore allowing more time to correct or prevent such failure. The micro-voids are nucleated at any discontinuity where a strain discontinuity like grain or subgrain boundaries, second phase particles and inclusions exists [11].

The fracture surfaces of the specimens during various ARB cycles are shown in Fig. 5. At 0-cycle ARB (before the ARB process), the specimens show dimples indicating the micro-void coalescence (MVC) mechanism of ductile fracture. The average initial void diameter (D_0) is 18 µm and 8.5 µm for ST-specimen and Aged-specimen, respectively. On the other hand, the average void diameter of the specimens after various ARB cycles is shown in Fig. 6. As shown in this figure, the average void diameter decreases with increasing the number of the ARB cycles in both the ST-ARB and the Aged-ARB specimens and the dimples are not as deep as at 0-cycle ARB. The size of the dimple on a fracture surface is governed by the number and distribution of micro-voids that are nucleated [11]. When the nucleation sites are few and widely spaced, the micro-voids grow to a large size before coalescing and the result is a fracture surface that contains large dimples. Small dimples are formed when numerous nucleating sites are activated and adjacent micro-voids join (coalesce) before they have an opportunity to grow to a larger size. Here, it is noteworthy that the average size of the dimples is larger in the ST-ARB specimen compared to the Aged-ARB specimen. The difference between the average size of the dimples can be related to the presence of fine precipitates in the Aged-ARB specimens because the Aged-ARB specimens have differet behavior compared to the ST-ARB specimen during the ARB process. This issue is clearly declared by Borhani et. al [6, 7]. The rate of the decrease in the average void diameter is larger in the ST-ARB specimen than that of the Aged-ARB specimen. On the other hand, the pre-existing

precipitates may effect on the average void diameter. As can be seen in Fig. 5, the void diameter of Aged-specimen is smaller than ST-specimen. This result shows that the ST-specimen and Aged-specimen have different behavior in fracture due to different starting microstructures. Also, Narasayya et. al reported that transgranular fracture observes due to the presence of the small second phase particles, which causes the formation of pockets of shallow dimples and microscopic voids of varying size [17]. They also reported that finer voids form due to the formation of ligament breaking between primary voids causing shear voiding between the primary voids and similar features observe in all aging condition in Al alloy [17]. This phenomenon requires further investigation. Ductile fractures can be detected before ARB process that has been already reported by Rezaei et. al [18].
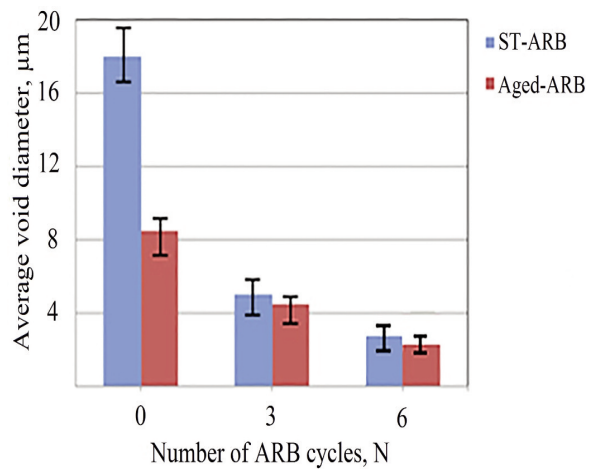
Figure 6. *The Average void diameter as a function of ARB cycles for 0, 3 and 6 cycles (N)*

ST-ARB   Aged-ARB
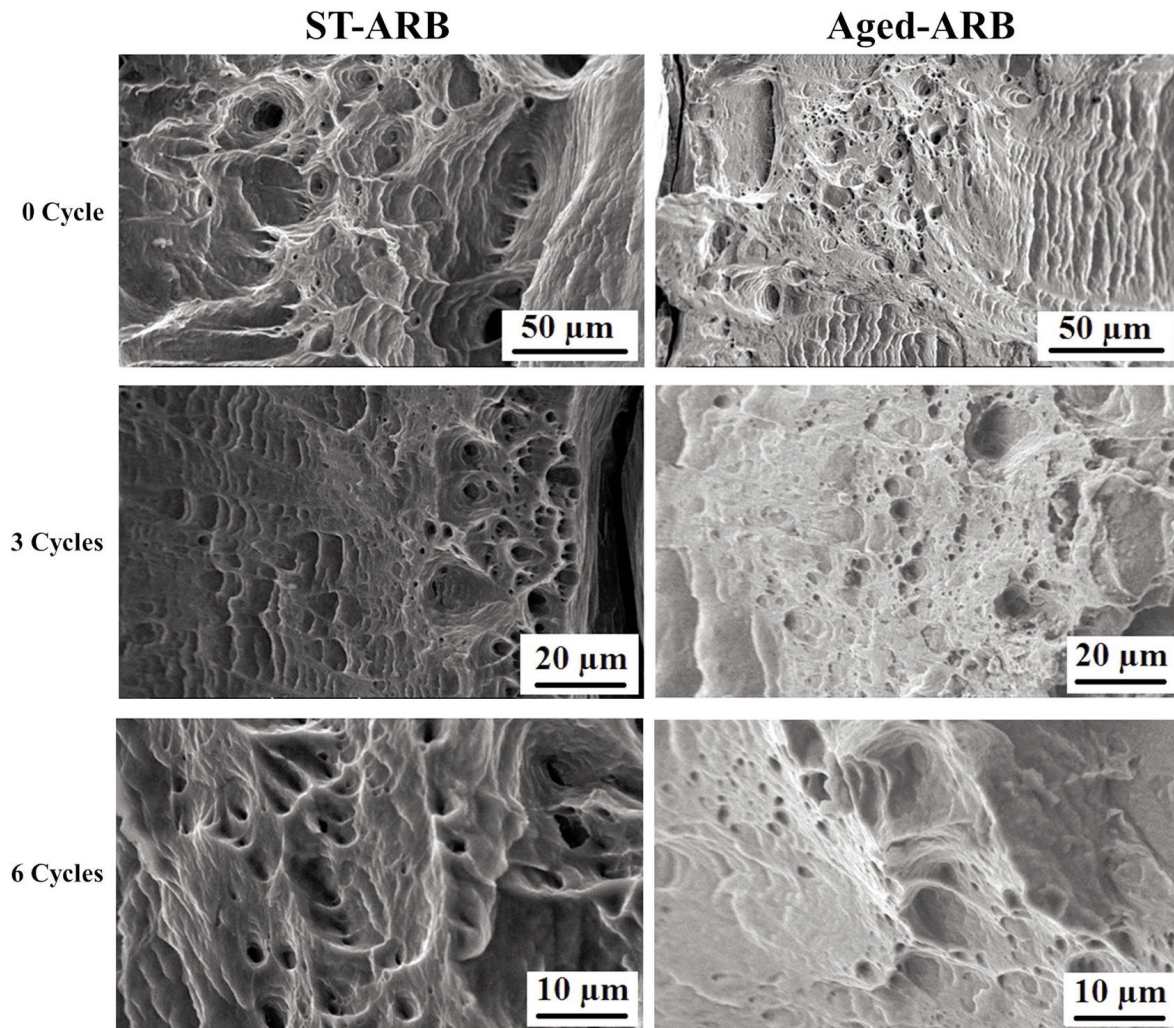
Figure 5. *Fracture surfaces of the specimens after various ARB cycles at different magnifications*

As shown in Fig.7 at mid-cycles and final cycles, the specimens show cleavage facets and river lines, that the river lines or the stress lines are steps between cleavage or parallel planes, which are always converged in the direction of local crack propagation. The river lines and cleavage facets are indicated by yellow and red arrows, respectively. This direction is normally observed pointing to inclusion, porosity, crack or second phase particle, which create stress concentration. Stress is therefore concentrated in front of these defects, initiating a crack of a critical size [11]. The propagation of this crack then finally causes the global failure with little plastic deformation.

From Fig. 5 and Fig. 7, the fracture mode is transgranular cleavage fracture in the Aged-specimen because the present of the precipitates after aging process. Transgranular cleavage fracture is usually associated with defects such as cracks, porosity, inclusions or second phase particles in which dislocations movement is obstructed [11]. It is thought that there are intersting diffrences aging and precipitation behaviors between conventially coarse grained materials and UFG materials [7]. As previously mentioned, with increasing the number of the ARB cycles, the size of dimples obviously decreases and the proportion of brittle fracture increases. On the other hand, with increasing the number of the ARB cycles, the brittle fracture is dominated.

4. Conclusion

The fracture surfaces after tensile test in the ST-ARB and the Aged-ARB specimens during ARB process up to 6 cycles were investigated. The main results are summarized as follows:

In the Aged-specimen were formed very fine precipitates after aging process. The mean grain size of the ST-ARB and the Aged-ARB specimens were 650 nm and 420 nm, respectively.

At 0-cycle ARB, the specimens showed dimples indicating the micro-void coalescence (MVC) mechanism of ductile fracture. On the other hand, the size of dimples decreased by increasing the number of the ARB cycles. Before the ARB process, ductile fracture was detected in both ST-ARB and Aged-ARB specimens. The fracture mode was transgranular cleavage fracture in the Aged-specimen.

With increasing the number of the ARB cycles, the size of dimples obviously decreased and the proportion of the brittle fracture increased.

The difference between fracture modes were seen in the ST-ARB and the Aged-ARB specimens was seen and it can be attributed to the pre-existing precipitates in the Aged-ARB specimen.
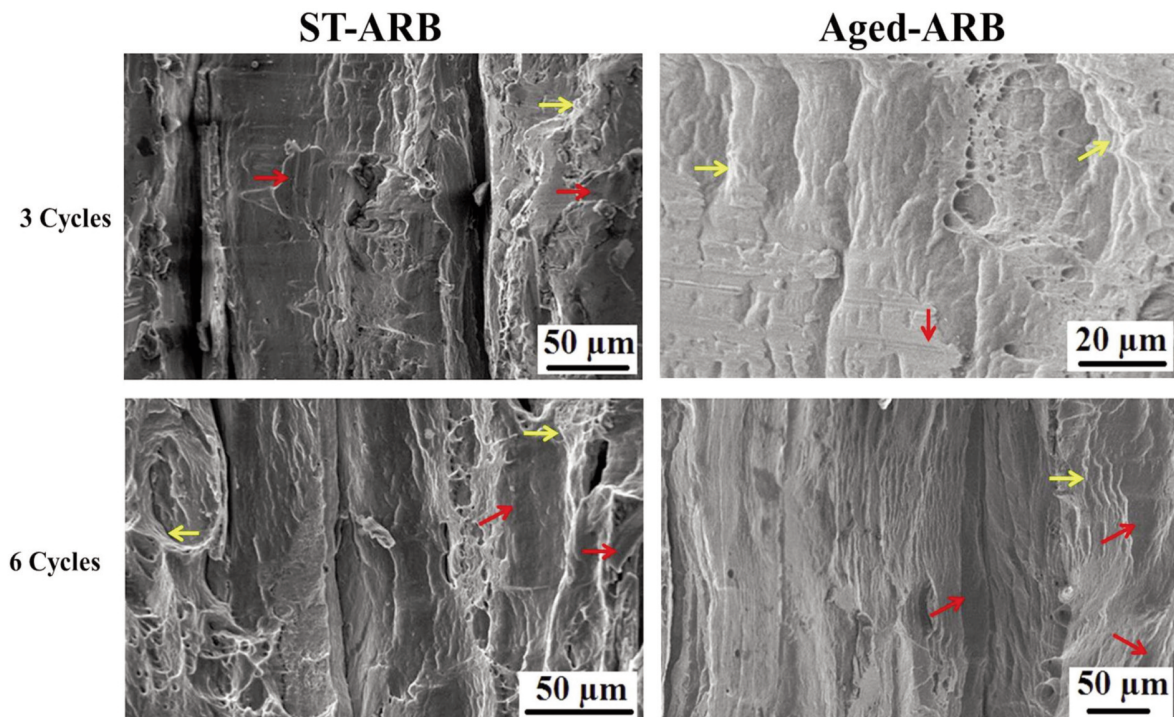
Figure 7. *Fracture surfaces of the specimens after various ARB cycles indicating river lines and cleavage facets at different magnifications*

References

[1]   A. Azushima , R. Kopp, A. Korhonen , D. Y. Yang, F. Micari, G. D. Lahoti, P. Groche, J. Yanagimoto, N. Tsuji, A. Rosochowski, A. Yanagida, Manufac. Tech., 57 (2) (2008) 716-735.

[2]   R. Z. Valiev, T. G. Langdon, Prog. Mater. Sci., 51 (7) (2006) 881-981.

[3]   A. P. Zhilyaev, T. G. Langdon, Prog. Mater. Sci., 53 (6) (2008) 893-979.

[4]   M. Richert, Q. Liu, N. Hansen, Mater. Sci. Eng., A 260 (1-2) (1999) 275-283.

[5]   Y. Saito, H. Utsunomiya, N. Tsuji, T. Sakai, Acta Mater., 47 (2) (1999) 579-583.

[6]   E. Borhani E, H. Jafarian, H. Adachi, D. Terada, N. Tsuji, Mater. Sci. Forum, 667-669 (2011) 211-216.

[7]   E. Borhani, H. Jafarian, D. Terada , H. Adachi, N. Tsuji, Mater. Trans., 53 (1) (2011) 72-80.

[8]   E. Borhani, H. Jafarian, A. Shibata, N. Tsuji, Mater. Trans., 53 (11) (2012) 1863-1869.

[9]   H. Pirgazi, A. Akbarzadeh, R. Petrov, L. Kestens, Mater. Sci. Eng. A, 497 (1-2) (2008) 132-138.

[10] S. H. Lee, Y. Saito, T. Sakai, H. Utsunomiya, Mater. Sci. Eng. A, 325 (1-2) (2002) 228-235.

[11] ASM Metals Handbook, Volume 12, Fractography.

[12] A. Biswas, D. J. Siegel, C. Wolverton, N. Seidman, Acta Mater., 59 (15) (2011) 6187-6204.

[13] B. G. Clark, I. M. Robertson, L. M. Dougherty, Mater. Res., 20 (2005) 1792-1801.

[14] X. Huang, N. Tsuji, N. Hansen, Y. Minamino, Mater. Sci. Eng. A, 340 (1-2) (2003) 265-271.

[15] T. Boukharouba, M. Elboujdaini, G. Pluvinage G, Damage and Fracture Mechanics: Failure Analysis of Engineering Materials and structures, Springer Verlag publishing, Dordrecht, The Netherland, 2009.

[16] M. A. Maleque, M. S. Salit, Materials Selection and Design, Springer publishing, Singapore, 2013.

[17] Ch.V.A. Narasayya, P. Rambabu, M.K. Mohan, Rahul Mitra, N. Eswara Prasad, Proc. Mater. Sci., 6 (2014) 322 –330.

[18] M. R. Rezaei, M. R. Toroghinejad, F. Ashrafizadeh, J. Mater. Proc. Tech., 211 (6) (2001) 1184-1190.